Scalable integrated single-photon source

Uppu, Ravitej; Pedersen, Freja T.; Wang, Ying; Olesen, Cecilie T.; Papon, Camille; Zhou, Xiaoyan; Midolo, Leonardo; Scholz, Sven; Wieck, Andreas D.; Ludwig, Arne; Lodahl, Peter

Citation for published version (APA):
Uppu, R., Pedersen, F. T., Wang, Y., Olesen, C. T., Papon, C., Zhou, X., ... Lodahl, P. (2020). Scalable integrated single-photon source. *Science Advances*, *6*(50), [8268]. https://doi.org/10.1126/sciadv.abc8268

OPTICS

Scalable integrated single-photon source

Ravitej Uppu[1]*, Freja T. Pedersen[1], Ying Wang[1], Cecilie T. Olesen[1], Camille Papon[1],
Xiaoyan Zhou[1], Leonardo Midolo[1], Sven Scholz[2], Andreas D. Wieck[2], Arne Ludwig[2], Peter Lodahl[1]*

Photonic qubits are key enablers for quantum information processing deployable across a distributed quantum network. An on-demand and truly scalable source of indistinguishable single photons is the essential component enabling high-fidelity photonic quantum operations. A main challenge is to overcome noise and decoherence processes to reach the steep benchmarks on generation efficiency and photon indistinguishability required for scaling up the source. We report on the realization of a deterministic single-photon source featuring near-unity indistinguishability using a quantum dot in an "on-chip" planar nanophotonic waveguide circuit. The device produces long strings of >100 single photons without any observable decrease in the mutual indistinguishability between photons. A total generation rate of 122 million photons per second is achieved, corresponding to an on-chip source efficiency of 84%. These specifications of the single-photon source are benchmarked for boson sampling and found to enable scaling into the regime of quantum advantage.

INTRODUCTION

Leveraging photonic quantum technology requires scalable hardware. A key enabling device is a high-quality and on-demand source of indistinguishable single photons with immediate use for quantum simulators (*1*), device-independent quantum communication (*2*), and memoryless quantum repeaters (*3*), or as a primer for multiphoton entanglement sources (*4*). Furthermore, single photons are the natural carriers of quantum information over extended distances, thereby providing a backbone for the quantum internet (*5*) by enabling fully secure quantum communication (*6*) and a modular approach to quantum computing (*7*, *8*).

An on-demand source of indistinguishable single photons is the major building block that can be realized either with a probabilistic source, which can be heralded and multiplexed to improve efficiency (*9*), or using a single quantum emitter coupled to a waveguide or cavity designed to collect the spontaneously emitted single photons. Substantial progress has been made with the latter approach by coupling quantum dots (QDs) to photonic nanostructures (*10*–*20*), and the governing fundamental processes determining performance have now clearly been identified including decoherence processes (*21*). Nonetheless, deterministic operation of a source of high-quality indistinguishable photons on a scalable platform has not yet been achieved, which is a key enabling step toward demonstrating quantum advantage with single photons (*22*, *23*). Quantum advantage has so far been reported with superconducting qubits (*24*), while the state of the art in photonics is the 20-photon experiment reported with a QD source (*25*). Deterministic and coherent operation of a photon source requires a number of simultaneous capabilities: (i) The QD must be deterministically and resonantly excited with a tailored optical pulse while eliminating the excess pump light without reducing the single-photon purity and efficiency, (ii) the emitted photon must be efficiently coupled to a single propagating mode, (iii) electrical control of the QD must be implemented to overcome efficiency loss due to emission into other QD charge states, and (iv) decoherence and noise

processes must be eliminated over the relevant time scale (*26*) to produce a scalable source of multiple indistinguishable photons.

In the present work, we implement all four functionalities in a single device, using a QD efficiently coupled to an electrically contacted planar photonic crystal waveguide membrane. We generate temporal strings of >100 single photons with pairwise photon indistinguishability exceeding 96%. Such a source coupled with an active temporal-to-spatial mode demultiplexer (*14*, *27*) will realize a paradigm shift for multiphoton experiments aimed at establishing photonic quantum advantage that requires more than 50 photons (*22*, *28*). In a recent breakthrough experiment, up to 20 photons were used in a boson sampling experiment (*25*); however, the photon indistinguishability was observed to decay over the 20-photon chain. This loss of coherence was also reported in previous experiments and only explained heuristically (*29*), and is likely a consequence of insufficient control of the QD charge environment leading to noise. Conceptually, the charge noise induces blinking of the QD that results in a loss of efficiency along with the broadening of the emission spectrum, which implies reduced coherence of the single-photon train. We implement electrical control of QDs coupled to photonic crystal waveguides through precise nanofabrication of low-noise electrical contacts that suppresses these detrimental effects. Our approach of combining high-quality semiconductor heterostructure growth together with advanced device design and nanofabrication is shown to robustly recover the transform-limited emission line shape (*30*), which is a key indicator for the generation of highly coherent single photons. In our improved source, we demonstrate coherence extending to at least 115 photons, as is proven by measuring the mutual degree of indistinguishability between photons emitted with a time delay approaching a microsecond. The source efficiency specifying the "on-chip" generation probability of indistinguishable single photons is $\eta_S = 84\%$, which is composed of 92% coupling of the dipole to the waveguide (the β factor), 95% efficient emission into the coherent zero-phonon line, 98% radiative decay efficiency, and >98% emission of the best-coupled of the two linear dipoles. Overall, we demonstrate the generation of 122 million photons per second in the waveguide, which is the main efficiency figure of merit that the present experiment targets. This massive photonic quantum resource is coupled off-chip and into an optical fiber, with an efficiency limited only by minor residual loss (4%) in

the waveguide and a chip-to-fiber outcoupling efficiency that reaches up to 82% with optimized grating outcouplers. The full details of the efficiency characterizations are presented in the Supplementary Materials in addition to an account of how to optimize external coupling efficiencies with already demonstrated methods to reach a fiber-coupled source with an overall efficiency of 78%. The improved source coherence will result in shorter runtimes for the validation of boson sampling in the quantum regime, thereby overcoming a major technological challenge. Our work lays a clear pathway for demonstrating quantum advantage in boson sampling with >50 photons using the source in combination with realistic low-loss optical networks and high-efficiency detectors.

RESULTS

Operational principle of the single-photon device

Figure 1 displays the device comprising epitaxially grown QDs embedded in a 180-nm-thin membrane (see section S1 for details on sample fabrication). The QD is excited with short optical pulses whereby an excitation in the QD can be deterministically prepared. The emitted single photons are channeled on-demand into a photonic crystal waveguide designed to control the local density of optical states such that an embedded QD emits with near-unity coupling efficiency (quantified by the β factor) into the waveguide (10). The collected photons are subsequently routed on-chip and directed to a tailored grating for highly efficient outcoupling to an optical fiber. The spatial separation between the excitation laser and the collection grating ensures that very high suppression of the pulsed resonant laser can be obtained without using any polarization filtering that could result in losses. Figure 2B shows an example of pulsed resonance fluorescence data that exhibit clear Rabi oscillation with highly suppressed laser background.

Demonstration of low-noise operation

The implementation of electrical contacts on the device (cf. Fig. 1) leads to a number of salient features: The embedded QDs can be electrically tuned, the charge state of the QD is stabilized so that emission only on the desired transition takes place, and spectral diffusion due to residual charge noise in the structures can be strongly suppressed. As a consequence, near–transform-limited optical line-
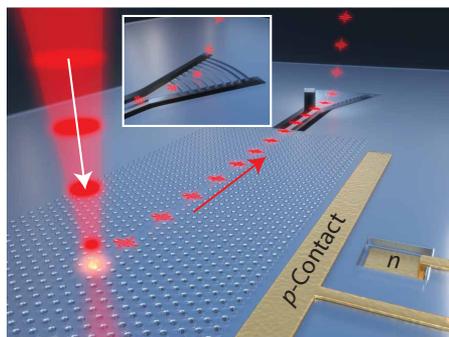

Fig. 1. Illustration of the single-photon source device. A QD embedded in a photonic crystal waveguide is excited using a pulsed laser at the resonance wavelength of the QD. The emitted single-photon train is coupled to the waveguide with near-unity efficiency and outcoupled from the device using a grating outcoupler (see inset). Metal electrical contacts (shown in gold) are used for applying a gate voltage across the QD embedded in the 180-nm-thin membrane.

widths can be achieved in the photonic nanostructures (19, 30, 31), which is essential for generating a scalable resource of indistinguishable photons as well as for more advanced applications of the system for photonic quantum gates and entanglement generation (21). Low-noise operation is demonstrated by exciting the QD with a tunable laser and collecting the resonance fluorescence. A typical measurement is displayed in Fig. 2A, where two distinct QD transitions (the two orthogonal dipoles of the neutral exciton) are visible and the excitation laser is clearly suppressed. A distinct Coulomb blockade regime is observed (32), meaning that the QD emits solely on the identified neutral exciton transition; i.e., blinking to other exciton complexes is fully suppressed. We observe a QD linewidth of ≈800 MHz, which is close to the transform limit, and the slight residual broadening is attributed to the slow time drift (1 to 10 ms) (33), which is irrelevant for the generation of indistinguishable photons over the nanosecond to microsecond time scales studied here.

Deterministic single-photon generation

Pulsed resonant excitation allows on-demand operation of the single-photon device. The QD was excited with 20-ps pulses, and clear Rabi oscillations are observed when increasing the excitation power (cf. Fig. 2B). The measured 10.4-MHz peak single-photon detection rate for a 145-MHz pump laser repetition rate is in good agreement with the estimated source efficiency (η_S = 84%; cf. table S1) for the nonoptimum setup efficiency of ≈8.4%, resulting in an in-fiber efficiency of 7%. We note that the setup efficiency can be readily optimized (see section S5.4) using off-the-shelf equipment and proven device designs to exceed 82%. Deterministic operation corresponds to excitation with a π pulse, where essentially background-free operation is observed with a very low single-photon impurity contribution of ξ < 0.007. Here, ξ is defined as the ratio of the laser background to the QD signal intensity. The single-photon purity is quantified in second-order photon correlation measurements (cf. data in Fig. 2D). We extract $g^{(2)}(0)$ = 0.015 ± 0.005, which can be further improved by engineering the resonant excitation pulse (34) or by implementing two-photon excitation schemes (35). Blinking of the source is essentially vanishing (cf. inset of Fig. 2D) up to time scales approaching milliseconds (data up to 50 μs shown). The photon emission dynamics is reproduced in Fig. 2C, where a radiative decay rate of γ = 2.89 ns^{-1} is extracted for the efficiently coupled dipole, which is enhanced by the Purcell effect of the waveguide leading to the large β factor (11).

Generation of long strings of indistinguishable photons

The indistinguishability of the temporal single-photon train is quantified through photon-photon interference experiments. In these measurements, two photons emitted at different times are interfered in an asymmetric interferometer with a variable time delay, as schematized in Fig. 3A. In this setup, we can measure the degree of indistinguishability between single photons emitted from the QD with time intervals $N\tau_p$, where τ_p is the laser repetition period and N is a positive integer. Figure 3C shows experimental data for the four representative values $N = \{1, 38, 76, 114\}$, where the latter corresponds to a maximum time delay between two photons of 786.6 ns. Figure 3B shows the recorded correlation histograms for N = 1 and N = 114 for the two cases where the interfering photons are co- and cross-polarized. The cross-polarized histogram serves as a reference measurement for extracting the degree of indistinguishability V after accounting for the setup imperfections (cf. section S4 for the analysis).
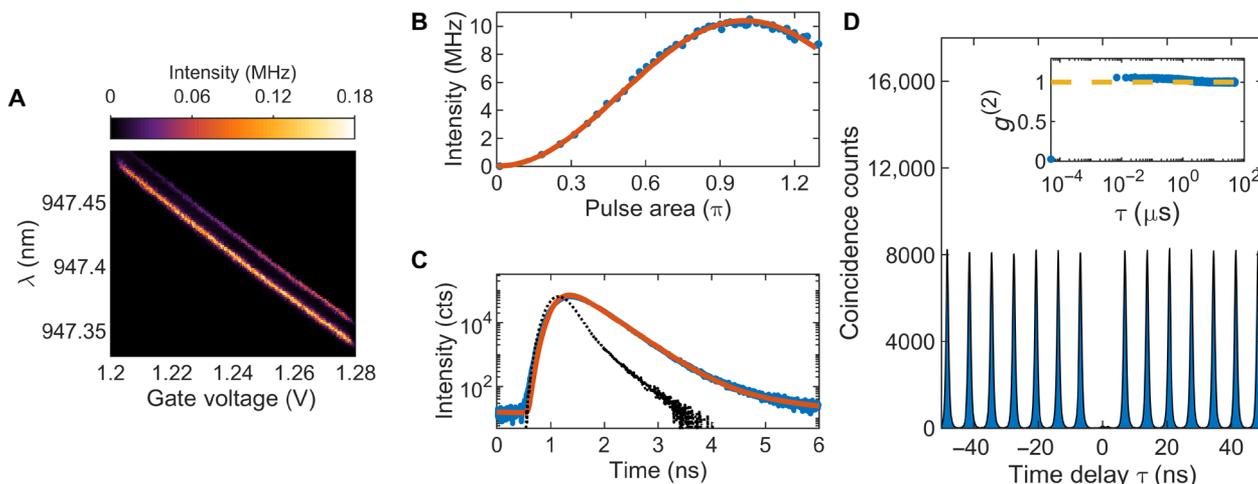
Fig. 2. Deterministic preparation of an excitation in the QD. (**A**) Resonance fluorescence measured from a QD in a photonic crystal waveguide weakly excited using a continuous-wave tunable diode laser. The two bright lines are the charge plateaus of the fine structure split neutral exciton. (**B**) Pulsed resonance fluorescence measured with the QD tuned on resonance ($V_g = 1.24$ V) and excited with a mode-locked laser with a pulse width of 20 ps. (**C**) Lifetime of the resonantly excited QD exhibiting a single-exponential decay with a radiative decay rate of $\gamma = 2.89$ ns^{-1}. The black dotted curve is the instrument response function of the measurement setup. cts, counts. (**D**) Measured coincidence counts of the single-photon source in a Hanbury Brown and Twiss interferometer under π pulse excitation showing a strongly suppressed peak at time delay $\tau = 0$. The small asymmetry visible as a double peak at $\tau = 0$ ns is a noise artifact in the bias electronics of the superconducting nanowire single-photon detectors. The inset shows the integrated coincidence counts under each peak over a time scale of 50 μs that highlights the minimal bunching observed.
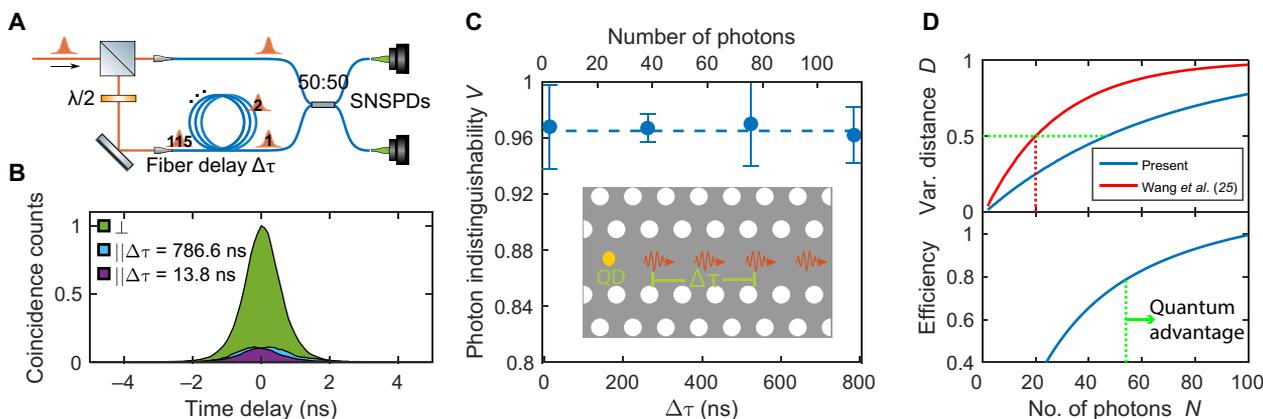

Fig. 3. Highly indistinguishable train of single photons. (**A**) Schematic of a fiber-based unbalanced Mach-Zehnder interferometer with a variable fiber delay line (delay time, $\Delta\tau$) in one arm used for Hong-Ou-Mandel interference measurements. SNSPD, superconducting nanowire single-photon detector. (**B**) Photon indistinguishability measured under π pulse excitation for photons generated with $\Delta\tau = 13.8$ ns and $\Delta\tau = 786.6$ ns and with the two input photons co- and cross-polarized by adjusting the half–wave plate in the fiber delay arm. (**C**) Photon indistinguishability between photon pairs in a temporal string of up to 115 photons reaching >96%, as illustrated by the interference of photon 1 with photons 2, 39, 77, and 115. (**D**) Estimate of boson sampling capabilities of QD sources. Top: Variational distance of an ideal boson sampler from the real scenario implemented with the present source (blue curve) and that from Wang *et al.* (*25*) (red curve). At a given *N*, higher trace distance requires more sampling events and hence longer time to validate the boson sampler, thereby inhibiting the scaling into quantum advantage. Bottom: Minimum source efficiency η_S required for validating boson sampling with *N* indistinguishable photons by detecting collision-free events in a fixed runtime of 30 days.

We find $V = (96 \pm 2)\%$ when accounting for the finite multiphoton probability discussed above, while $V = (93 \pm 2)\%$ is directly recorded. The minor amount of distinguishability can be attributed to the residual elastic phonon scattering (*36*), which is the fundamental decoherence process that determines the performance of QD single-photon sources. The degree of indistinguishability due to phonon scattering is dependent on the photonic nanostructure owing to the quantized phonon modes (*37*) and the sample temperature. At the sample temperature of 1.6 K, in our measurements, the expected indistinguishability is ≈98% in the photonic crystal membrane, where

the experimental values are limited by the finite resolution of the interferometer. We find the photon indistinguishability to remain over 96% for delays corresponding to 115 photons (cf. Fig. 3C), which is key for the applicability of the source to reach quantum advantage, as benchmarked below.

DISCUSSION
Scalable boson sampling experiments using QD sources use active switching of the temporal string of single photons into separate

optical modes, thereby realizing a multiphoton source. Even a small degree of distinguishability of photons can strongly influence the scalability of boson sampling into the quantum advantage regime (*38*). The impact of the improved source coherence on boson sampling can be quantified using the variational distance *D* of boson sampling, which is the statistical distance between the probability distributions of photon correlations, implemented using the partially distinguishable photon source and an ideal source (*39*, *40*). For distinguishable photons in a Haar unitary optical network, $D \approx 1$ for large *N*. Therefore, validation of boson sampling against the classically simulatable case of distinguishable photons requires $D < 1$, with larger *D* demanding higher number of multiphoton detection events. Better source coherence, i.e., higher pairwise indistinguishability across the string, results in a lower *D* for any *N*-photon boson sampling, as shown in the top panel of Fig. 3D. At the comparable *D* as the 20-photon boson sampling in (*25*), the better source coherence reported here enables boson sampling with 54 photons (see section S6 for details). The bottom panel of Fig. 3D depicts the required efficiency of the source for boson sampling versus the number of photons for a technologically feasible operation time of 30 days. We find that reaching the regime of quantum advantage requires a QD source efficiency, $\eta_S > 78\%$, where we include the finite transmittances of the demultiplexing circuit and the boson sampling network as well as the nonunity detector efficiencies reported in (*25*). Given the demonstrated $\eta_S > 84\%$, an on-chip boson sampling circuit could be pursued. However, state-of-the-art boson sampling is realized using bulk optics in a tabletop setup. This requires efficient outcoupling of photons from the chip and into a single-mode optical fiber. The setup efficiency for fiber outcoupling the photons reaches >85%, following the steps discussed in section S5.4. By improving the on-chip source efficiency to >92%, which is readily possible by proper spatial alignment of the QD in the waveguide, the overall efficiency required in a tabletop boson sampling experiment demonstrating quantum advantage can be reached (cf. the Supplementary Materials). We emphasize that near-unity indistinguishability extending over the whole string of generated photons, which is achieved in our low-noise devices, is essential for scaling up to reach the quantum advantage threshold. We note that given the high-quality photonic resource, these runtimes could be further improved using the Aaronson-Brod model of boson sampling (*41*).

We have presented a scalable single-photon source based on a QD in a photonic waveguide, meeting the very strict requirements needed for demonstrating quantum advantage of photonic qubits. Reaching quantum advantage is a crucial first step toward advanced quantum simulators and computers, providing a clear benchmark on the metrics for quantum hardware. Notably, these benchmarks are universal; i.e., they are also essential figures of merit for more advanced photonic quantum resources produced with QD sources than the independent photons required for boson sampling. Consequently, our work is expected to spur diverse interest toward application of QD sources for deterministic photonic quantum gates, multiphoton entanglement generation, and nonlinear quantum optics.

MATERIALS AND METHODS
Sample fabrication
The samples are fabricated on a gallium arsenide (GaAs) membrane grown by molecular beam epitaxy on a (100) GaAs substrate. The substrate is prepared for growth using an aluminum arsenide (AlAs)/GaAs superlattice followed by the growth of a 1150-nm-thick $Al_{0.75}Ga_{0.25}As$ sacrificial layer. Subsequently, a 180-nm-thin GaAs membrane containing indium arsenide (InAs) QDs is grown on top of the sacrificial layer. The membrane constitutes an ultrathin *p-i-n* diode (cf. fig. S1A for the heterostructure design). The first step in creating the nanostructures is the fabrication of the electrical contacts to the *p*-doped and *n*-doped layers. Reactive-ion etching in a BCl_3/Ar chemistry is used to open vias to the *n* layer, and Ni/Ge/Au/Ni/Au contacts are deposited by electron beam physical vapor deposition and annealed at 430°C. Subsequently, Cr/Au pads are deposited on the surface to realize ohmic *p*-type contacts. The nanostructuring is then carried out using a soft mask–based process described in (*42*). The residual polymer from the soft mask is removed by dipping the sample in *N*-methyl-pyrrolidone at 70°C. The sacrificial layer is then removed using wet etching using hydrofluoric acid to release the membrane.

Experimental setup
The sample is cooled to 1.6 K in a cryostat with optical and electrical access. The QD is excited from the top of the chip using a wide field-of-view confocal microscope with a high numerical aperture objective (NA = 0.81) (cf. fig. S4A). The emission from the QD is collected at the grating outcoupler through the same objective and imaged onto a single-mode optical fiber. The excitation and collection paths are separated at a 5:95 (reflection/transmission) beam splitter, with the 95% transmission path for collection. A set of quarter– and half–wave plates in the excitation path allow polarization control of the excitation laser. The QD emission collected in the fiber is spectrally filtered using a 3-GHz linewidth etalon (free spectral range: 100 GHz) to suppress the emission in the phonon sideband. The intensity of the spectrally filtered emission is measured using a fiber-coupled superconducting nanowire single-photon detector. The bias voltage across the QD is tuned using a low-noise high-resolution DC voltage source.

SUPPLEMENTARY MATERIALS
Supplementary material for this article is available at http://advances.sciencemag.org/cgi/content/full/6/50/eabc8268/DC1

REFERENCES AND NOTES
1. A. Aspuru-Guzik, P. Walther, Photonic quantum simulators. *Nat. Phys.* **8**, 285–291 (2012).
2. J. Kołodyński, A. Máttar, P. Skrzypczyk, E. Woodhead, D. Cavalcanti, K. Banaszek, A. Acín, Device-independent quantum key distribution with single-photon sources. *Quantum* **4**, 260 (2020).
3. J. Borregaard, H. Pichler, T. Schröder, M. D. Lukin, P. Lodahl, A. S. Sørensen, One-way quantum repeater based on near-deterministic photon-emitter interfaces. *Phys. Rev. X* **10**, 021071 (2020).
4. N. H. Lindner, T. Rudolph, Proposal for pulsed on-demand sources of photonic cluster state strings. *Phys. Rev. Lett.* **103**, 113602 (2009).
5. H. J. Kimble, The quantum internet. *Nature* **453**, 1023–1030 (2008).
6. S. Wehner, D. Elkouss, R. Hanson, Quantum internet: A vision for the road ahead. *Science* **362**, eaam9288 (2018).
7. T. Rudolph, Why I am optimistic about the silicon-photonic route to quantum computing. *APL Photonics* **2**, 030901 (2017).
8. C. Monroe, J. Kim, Scaling the ion trap quantum processor. *Science* **339**, 1164–1169 (2013).
9. F. Kaneda, P. G. Kwiat, High-efficiency single-photon generation via large-scale active time multiplexing. *Sci. Adv.* **5**, eaaw8586 (2019).
10. M. Arcari, I. Söllner, A. Javadi, S. Lindskov Hansen, S. Mahmoodian, J. Liu, H. Thyrrestrup, E. H. Lee, J. D. Song, S. Stobbe, P. Lodahl, Near-unity coupling efficiency of a quantum emitter to a photonic crystal waveguide. *Phys. Rev. Lett.* **113**, 093603 (2014).
11. P. Lodahl, S. Mahmoodian, S. Stobbe, Interfacing single photons and single quantum dots with photonic nanostructures. *Rev. Mod. Phys.* **87**, 347–400 (2015).

12. N. Somaschi, V. Giesz, L. De Santis, J. C. Loredo, M. P. Almeida, G. Hornecker, S. L. Portalupi, T. Grange, C. Antón, J. Demory, C. Gómez, I. Sagnes, N. D. Lanzillotti-Kimura, A. Lemaître, A. Auffeves, A. G. White, L. Lanco, P. Senellart, Near-optimal single-photon sources in the solid state. *Nat. Photonics* **10**, 340–345 (2016).

13. S. Unsleber, Y.-M. He, S. Gerhardt, S. Maier, C.-Y. Lu, J.-W. Pan, N. Gregersen, M. Kamp, C. Schneider, S. Höfling, Highly indistinguishable on-demand resonance fluorescence photons from a deterministic quantum dot micropillar device with 74% extraction efficiency. *Opt. Express* **24**, 8539–8546 (2016).

14. H. Wang, Y. He, Y.-H. Li, Z.-E. Su, B. Li, H.-L. Huang, X. Ding, M.-C. Chen, C. Liu, J. Qin, J.-P. Li, Y.-M. He, C. Schneider, M. Kamp, C.-Z. Peng, S. Höfling, C.-Y. Lu, J.-W. Pan, High-efficiency multiphoton boson sampling. *Nat. Photonics* **11**, 361–365 (2017).

15. Y.-M. He, J. Liu, S. Maier, M. Emmerling, S. Gerhardt, M. Davanço, K. Srinivasan, C. Schneider, S. Höfling, Deterministic implementation of a bright, on-demand single-photon source with near-unity indistinguishability via quantum dot imaging. *Optica* **4**, 802–808 (2017).

16. G. Kiršanskė, H. Thyrrestrup, R. S. Daveau, C. L. Dreeßen, T. Pregnolato, L. Midolo, P. Tighineanu, A. Javadi, S. Stobbe, R. Schott, A. Ludwig, A. D. Wieck, S. I. Park, J. D. Song, A. V. Kuhlmann, I. Söllner, M. C. Löbl, R. J. Warburton, P. Lodahl, Indistinguishable and efficient single photons from a quantum dot in a planar nanobeam waveguide. *Phys. Rev. B* **96**, 165306 (2017).

17. F. Liu, A. J. Brash, J. O'Hara, L. M. P. P. Martins, C. L. Phillips, R. J. Coles, B. Royall, E. Clarke, C. Bentham, N. Prtljaga, I. E. Itskevich, L. R. Wilson, M. S. Skolnick, A. M. Fox, High Purcell factor generation of indistinguishable on-chip single photons. *Nat. Nanotechnol.* **13**, 835–840 (2018).

18. H. Wang, Y.-M. He, T.-H. Chung, H. Hu, Y. Yu, S. Chen, X. Ding, M.-C. Chen, J. Qin, X. Yang, R.-Z. Liu, Z.-C. Duan, J.-P. Li, S. Gerhardt, K. Winkler, J. Jurkat, L.-J. Wang, N. Gregersen, Y.-H. Huo, Q. Dai, S. Yu, S. Höfling, C.-Y. Lu, J.-W. Pan, Towards optimal single-photon sources from polarized microcavities. *Nat. Photonics* **13**, 770–775 (2019).

19. H. Thyrrestrup, G. Kiršanskė, H. Le Jeannic, T. Pregnolato, L. Zhai, L. Raahauge, L. Midolo, N. Rotenberg, A. Javadi, R. Schott, A. D. Wieck, A. Ludwig, M. C. Löbl, I. Söllner, R. J. Warburton, P. Lodahl, Quantum optics with near-lifetime-limited quantum-dot transitions in a nanophotonic waveguide. *Nano Lett.* **18**, 1801–1806 (2018).

20. R. Uppu, H. T. Eriksen, H. Thyrrestrup, A. D. Uğurlu, Y. Wang, S. Scholz, A. D. Wieck, A. Ludwig, M. C. Löbl, R. J. Warburton, P. Lodahl, L. Midolo, On-chip deterministic operation of quantum dots in dual-mode waveguides for a plug-and-play single-photon source. *Nat. Commun.* **11**, 3782 (2020).

21. P. Lodahl, Quantum-dot based photonic quantum networks. *Quantum Sci. Technol.* **3**, 013001 (2018).

22. J. Preskill, Quantum computing in the NISQ era and beyond. *Quantum* **2**, 79 (2018).

23. S. Aaronson, L. Chen, Complexity-theoretic foundations of quantum supremacy experiments. arXiv:1612.05903 (2016).

24. F. Arute, K. Arya, R. Babbush, D. Bacon, J. C. Bardin, R. Barends, R. Biswas, S. Boixo, F. G. S. L. Brandao, D. A. Buell, B. Burkett, Y. Chen, Z. Chen, B. Chiaro, R. Collins, W. Courtney, A. Dunsworth, E. Farhi, B. Foxen, A. Fowler, C. Gidney, M. Giustina, R. Graff, K. Guerin, S. Habegger, M. P. Harrigan, M. J. Hartmann, A. Ho, M. Hoffmann, T. Huang, T. S. Humble, S. V. Isakov, E. Jeffrey, Z. Jiang, D. Kafri, K. Kechedzhi, J. Kelly, P. V. Klimov, S. Knysh, A. Korotkov, F. Kostritsa, D. Landhuis, M. Lindmark, E. Lucero, D. Lyakh, S. Mandrà, J. R. McClean, M. McEwen, A. Megrant, X. Mi, K. Michielsen, M. Mohseni, J. Mutus, O. Naaman, M. Neeley, C. Neill, M. Y. Niu, E. Ostby, A. Petukhov, J. C. Platt, C. Quintana, E. G. Rieffel, P. Roushan, N. C. Rubin, D. Sank, K. J. Satzinger, V. Smelyanskiy, K. J. Sung, M. D. Trevithick, A. Vainsencher, B. Villalonga, T. White, Z. J. Yao, P. Yeh, A. Zalcman, H. Neven, J. M. Martinis, Quantum supremacy using a programmable superconducting processor. *Nature* **574**, 505–510 (2019).

25. H. Wang, J. Qin, X. Ding, M.-C. Chen, S. Chen, X. You, Y.-M. He, X. Jiang, L. You, Z. Wang, C. Schneider, J. J. Renema, S. Höfling, C.-Y. Lu, J.-W. Pan, Boson sampling with 20 input photons and a 60-mode interferometer in a 10^{14}-dimensional Hilbert space. *Phys. Rev. Lett.* **123**, 250503 (2019).

26. A. V. Kuhlmann, J. Houel, A. Ludwig, L. Greuter, D. Reuter, A. D. Wieck, M. Poggio, R. J. Warburton, Charge noise and spin noise in a semiconductor quantum device. *Nat. Phys.* **9**, 570–575 (2013).

27. T. Hummel, C. Ouellet-Plamondon, E. Ugur, I. Kulkova, T. Lund-Hansen, M. A. Broome, R. Uppu, P. Lodahl, Efficient demultiplexed single-photon source with a quantum dot coupled to a nanophotonic waveguide. *Appl. Phys. Lett.* **115**, 021102 (2019).

28. A. P. Lund, M. J. Bremner, T. C. Ralph, Quantum sampling problems, BosonSampling and quantum supremacy. *npj Quantum Inf.* **3**, 15 (2017).

29. H. Wang, Z.-C. Duan, Y.-H. Li, S. Chen, J.-P. Li, Y.-M. He, M.-C. Chen, Y. He, X. Ding, C.-Z. Peng, C. Schneider, M. Kamp, S. Höfling, C.-Y. Lu, J.-W. Pan, Near-transform-limited single photons from an efficient solid-state quantum emitter. *Phys. Rev. Lett.* **116**, 213601 (2016).

30. F. T. Pedersen, Y. Wang, C. T. Olesen, S. Scholz, A. D. Wieck, A. Ludwig, M. C. Löbl, R. J. Warburton, L. Midolo, R. Uppu, P. Lodahl, Near transform-limited quantum dot linewidths in a broadband photonic crystal waveguide. *ACS Photonics* **7**, 2343–2349 (2020).

31. A. V. Kuhlmann, J. H. Prechtel, J. Houel, A. Ludwig, D. Reuter, A. D. Wieck, R. J. Warburton, Transform-limited single photons from a single quantum dot. *Nat. Commun.* **6**, 8204 (2015).

32. R. J. Warburton, Single spins in self-assembled quantum dots. *Nat. Mater.* **12**, 483–493 (2013).

33. J. Liu, K. Konthasinghe, M. Davanço, J. Lawall, V. Anant, V. Verma, R. Mirin, S. W. Nam, J. D. Song, B. Ma, Z. S. Chen, H. Q. Ni, Z. C. Niu, K. Srinivasan, Single self-assembled InAs/GaAs quantum dots in photonic nanostructures: The role of nanofabrication. *Phys. Rev. Appl.* **9**, 064019 (2018).

34. S. Das, L. Zhai, M. Čepulskovskis, A. Javadi, S. Mahmoodian, P. Lodahl, A. S. Sørensen, A wave-function ansatz method for calculating field correlations and its application to the study of spectral filtering and quantum dynamics of multi-emitter systems. arXiv:1912.08303 (2019).

35. L. Schweickert, K. D. Jöns, K. D. Zeuner, S. F. Covre da Silva, H. Huang, T. Lettner, M. Reindl, J. Zichi, R. Trotta, A. Rastelli, V. Zwiller, On-demand generation of background-free single photons from a solid-state source. *Appl. Phys. Lett.* **112**, 093106 (2018).

36. P. Tighineanu, C. L. Dreeßen, C. Flindt, P. Lodahl, A. S. Sørensen, Phonon decoherence of quantum dots in photonic structures: Broadening of the zero-phonon line and the role of dimensionality. *Phys. Rev. Lett.* **120**, 257401 (2018).

37. C. L. Dreeßen, C. Oullet-Plamondon, P. Tighineanu, X. Zhou, L. Midolo, A. S. Sørensen, P. Lodahl, Suppressing phonon decoherence of high performance single-photon sources in nanophotonic waveguides. *Quantum Sci. Technol.* **4**, 015003 (2019).

38. J. J. Renema, A. Menssen, W. R. Clements, G. Triginer, W. S. Kolthammer, I. A. Walmsley, Efficient classical algorithm for boson sampling with partially distinguishable photons. *Phys. Rev. Lett.* **120**, 220502 (2018).

39. M. C. Tichy, Sampling of partially distinguishable bosons and the relation to the multidimensional permanent. *Phys. Rev. A* **91**, 022316 (2015).

40. V. S. Shchesnovich, Tight bound on the trace distance between a realistic device with partially indistinguishable bosons and the ideal BosonSampling. *Phys. Rev. A* **91**, 063842 (2015).

41. S. Aaronson, D. J. Brod, BosonSampling with lost photons. *Phys. Rev. A* **93**, 012335 (2016).

42. L. Midolo, T. Pregnolato, G. Kiršanskė, S. Stobbe, Soft-mask fabrication of gallium arsenide nanomembranes for integrated quantum photonics. *Nanotechnology* **26**, 484002 (2015).

43. M. C. Löbl, S. Scholz, I. Söllner, J. Ritzmann, T. Denneulin, A. Kovács, B. E. Kardynał, A. D. Wieck, A. Ludwig, R. J. Warburton, Excitons in InGaAs quantum dots without electron wetting layer states. *Commun. Phys.* **2**, 93 (2019).

44. A. Javadi, I. Söllner, M. Arcari, S. L. Hansen, L. Midolo, S. Mahmoodian, G. Kiršanskė, T. Pregnolato, E. H. Lee, J. D. Song, S. Stobbe, P. Lodahl, Single-photon non-linear optics with a quantum dot in a waveguide. *Nat. Commun.* **6**, 8655 (2015).

45. C. Santori, D. Fattal, J. Vučković, G. S. Solomon, Y. Yamamoto, Indistinguishable photons from a single-photon device. *Nature* **419**, 594–597 (2002).

46. E. M. G. Ruiz, thesis, University of Copenhagen (2019).

47. S. Kako, C. Santori, K. Hoshino, S. Götzinger, Y. Yamamoto, Y. Arakawa, A gallium nitride single-photon source operating at 200 K. *Nat. Mater.* **5**, 887–892 (2006).

48. J. Johansen, B. Julsgaard, S. Stobbe, J. M. Hvam, P. Lodahl, Probing long-lived dark excitons in self-assembled quantum dots. *Phys. Rev. B* **81**, 081304(R) (2010).

49. M. Davanço, C. S. Hellberg, S. Ates, A. Badolato, K. Srinivasan, Multiple time scale blinking in InAs quantum dot single-photon sources. *Phys. Rev. B* **89**, 161303(R) (2014).

50. X. Zhou, I. Kulkova, T. Lund-Hansen, S. L. Hansen, P. Lodahl, L. Midolo, High-efficiency shallow-etched grating on GaAs membranes for quantum photonic applications. *Appl. Phys. Lett.* **113**, 251103 (2018).

51. L. Scarpelli, B. Lang, F. Masia, D. M. Beggs, E. A. Muljarov, A. B. Young, R. Oulton, M. Kamp, S. Höfling, C. Schneider, W. Langbein, 99% beta factor and directional coupling of quantum dots to fast light in photonic crystal waveguides determined by spectral imaging. *Phys. Rev. B* **100**, 035311 (2019).

52. M. Pu, L. Liu, H. Ou, K. Yvind, J. M. Hvam, Ultra-low-loss inverted taper coupler for silicon-on-insulator ridge waveguide. *Opt. Commun.* **283**, 3678–3682 (2010).

53. T. G. Tiecke, K. P. Nayak, J. D. Thompson, T. Peyronel, N. P. de Leon, V. Vuletić, M. D. Lukin, Efficient fiber-optical interface for nanophotonic devices. *Optica* **2**, 70–75 (2015).

54. S. Aaronson, A. Arkhipov, The computational complexity of linear optics. *Theor. Comput.* **9**, 143–252 (2013).

55. M. Jerrum, A. Sinclair, E. Vigoda, A polynomial-time approximation algorithm for the permanent of a matrix with nonnegative entries. *J. ACM* **51**, 671–697 (2004).

56. A. Arkhipov, BosonSampling is robust against small errors in the network matrix. *Phys. Rev. A* **92**, 062326 (2015).

57. V. S. Shchesnovich, Sufficient condition for the mode mismatch of single photons for scalability of the boson-sampling computer. *Phys. Rev. A* **89**, 022333 (2014).

58. P. P. Rohde, Boson sampling with photons of arbitrary spectral structure. *Phys. Rev. A* **91**, 012307 (2015).

59. H. Wang, W. Li, X. Jiang, Y.-M. He, Y.-H. Li, X. Ding, M.-C. Chen, J. Qin, C.-Z. Peng, C. Schneider, M. Kamp, W.-J. Zhang, H. Li, L.-X. You, Z. Wang, J. P. Dowling, S. Höfling,

C.-Y. Lu, J.-W. Pan, Toward scalable boson sampling with photon loss. *Phys. Rev. Lett.* **120**, 230502 (2018).

60. S. Rahimi-Keshari, T. C. Ralph, C. M. Caves, Sufficient conditions for efficient classical simulation of quantum optics. *Phys. Rev. X* **6**, 021039 (2016).

61. A. Neville, C. Sparrow, R. Clifford, E. Johnston, P. M. Birchall, A. Montanaro, A. Laing, Classical boson sampling algorithms with superior performance to near-term experiments. *Nat. Phys.* **13**, 1153–1157 (2017).

62. P. Clifford, R. Clifford, The classical complexity of boson sampling, in *Proceedings of the Twenty-Ninth Annual ACM-SIAM Symposium on Discrete Algorithms* (SIAM, 2018), pp. 146–155.

63. M. Oszmaniec, D. J. Brod, Classical simulation of photonic linear optics with lost particles. *New J. Phys.* **20**, 092002 (2018).

64. R. García-Patrón, J. J. Renema, V. S. Shchesnovich, Simulating boson sampling in lossy architectures. *Quantum* **3**, 169 (2019).

65. A. E. Moylett, R. García-Patrón, J. J. Renema, P. S. Turner, Classically simulating near-term partially-distinguishable and lossy boson sampling. *Quantum Sci. Technol.* **5**, 015001 (2019).

66. Introducing Summit, www.olcf.ornl.gov/summit/ [accessed 3 April 2020].

67. M. Ferrante, N. Frigo, A note on the coupon-collector's problem with multiple arrivals and the random sampling. arXiv:1209.2667 (2012).

68. I. Esmaeil Zadeh, J. W. N. Los, R. B. M. Gourgues, V. Steinmetz, G. Bulgarini, S. M. Dobrovolskiy, V. Zwiller, S. N. Dorenbos, Single-photon detectors combining high efficiency, high detection rates, and ultra-high timing resolution. *APL Photonics* **2**, 111301 (2017).

69. A. Arkhipov, G. Kuperberg, The bosonic birthday paradox. *Geom. Topol. Monogr.* **18**, 1–7 (2012).

70. N. Spagnolo, C. Vitelli, M. Bentivegna, D. J. Brod, A. Crespi, F. Flamini, S. Giacomini, G. Milani, R. Ramponi, P. Mataloni, R. Osellame, E. F. Galvão, F. Sciarrino, Experimental validation of photonic boson sampling. *Nat. Photonics* **8**, 615–620 (2014).

71. J. Carolan, J. D. A. Meinecke, P. J. Shadbolt, N. J. Russell, N. Ismail, K. Wörhoff, T. Rudolph, M. G. Thompson, J. L. O'Brien, J. C. F. Matthews, A. Laing, On the experimental verification of quantum complexity in linear optics. *Nat. Photonics* **8**, 621–626 (2014).

72. K. Liu, A. P. Lund, Y.-J. Gu, T. C. Ralph, A certification scheme for the boson sampler. *J. Opt. Soc. Am. B* **33**, 1835–1841 (2016).

73. I. Agresti, N. Viggianiello, F. Flamini, N. Spagnolo, A. Crespi, R. Osellame, N. Wiebe, F. Sciarrino, Pattern recognition techniques for boson sampling validation. *Phys. Rev. X* **9**, 011013 (2019).

Science Advances

Scalable integrated single-photon source

Ravitej Uppu, Freja T. Pedersen, Ying Wang, Cecilie T. Olesen, Camille Papon, Xiaoyan Zhou, Leonardo Midolo, Sven Scholz, Andreas D. Wieck, Arne Ludwig and Peter Lodahl

ARTICLE TOOLS	http://advances.sciencemag.org/content/6/50/eabc8268
SUPPLEMENTARY MATERIALS	http://advances.sciencemag.org/content/suppl/2020/12/07/6.50.eabc8268.DC1
REFERENCES	This article cites 67 articles, 3 of which you can access for free http://advances.sciencemag.org/content/6/50/eabc8268#BIBL
PERMISSIONS	http://www.sciencemag.org/help/reprints-and-permissions

Use of this article is subject to the Terms of Service